Radio Science, Volume 5, Number 6, pages 917–924. June 1970

A proposed wide-band satellite transmission experiment

E. J. Fremouw and A. A. Burns

Radio Physics Laboratory, Stanford Research Institute
Menlo Park, California 94025

(Received November 20, 1969.)

An experiment has been proposed, for the early 1970's, for the purpose of obtaining data on ionospheric and tropospheric effects on wide-band trans-atmospheric transmission. It is desired to radiate three combs (each composed of seven to ten highly stable, phase-coherent CW signals) from a geostationary satellite and to monitor the amplitude and phase of the signals in considerable detail. The tones would be grouped at *S* band, *L* band, and UHF, with group bandwidths and frequency spacings set to measure the mean dispersion and second-order parameters of the random part of the channel. One CW signal would be transmitted at HF and one at VHF to provide a comparative link with the existing collection of scintillation data obtained by various workers. Some multiple-antenna observations are desired so that spatial coherence questions can also be attacked. It is hoped that observations will be made through the equatorial, midlatitude, and auroral ionosphere.

INTRODUCTION

The development of communications and radar systems has resulted in ever increasing bandwidths. For systems that involve trans-atmospheric transmission (such as communication satellites and sophisticated radars of the future) the atmosphere probably sets the ultimate bandwidth limit. In the UHF and lower microwave bands, ionospheric dispersion probably dictates the final limit. At higher frequencies, spatial inhomogeneities in the ionosphere and troposphere may be more important.

Scattering from ionospheric irregularities will also influence the lower frequencies. The irregular phase shifts and amplitude fluctuations attendant to the scattering will decrease the band over which signal frequency components retain their initial relationships, representing a decreased 'correlation bandwidth.' Even slight partial decorrelation may be a problem for some systems. The usable bandwidth limit set by scattering is probably more variable and less predictable than that set by dispersion, because the irregular structure of the ionosphere may be more variable and is less understood than its gross characteristics.

Scattering from ionospheric and tropospheric irregularities also limits the gain and resolution we may expect from large-aperture antennas. On frequencies through low UHF, we may expect occasional nearly complete loss of signal correlation between sufficiently separated antenna elements; this phenomenon would limit the achievable angular resolution of the antenna. Such occurrences have been observed at VHF through the equatorial ionosphere [*Koster*, 1958; *Coates and Golden*, 1968] and at VHF and UHF through the auroral ionosphere [*Little et al.*, 1962; *Flood*, 1963; *Fremouw and Lansinger*, 1968]. At higher frequencies, partial decorrelation across a large-aperture antenna may occur; this decorrelation would lead to reduced performance.

Existing knowledge about the atmosphere and its irregular structure permits us to make the above qualitative statements about bandwidth and aperture limitation. It also allows us to make order-of-magnitude estimates of the likely limitations, at least in some average sense. However, our state of understanding of atmospheric processes (such as the formation of ionospheric irregularities) precludes detailed quantitative calculations of the limits as functions of observing location, time, and pertinent solar-geophysical conditions. This paper describes an experiment designed to measure the bandwidth and aperture limits directly.

To provide a truly trans-atmospheric experiment and to allow extended continuous observations from a given ground station, it is desired to transmit signals from a geostationary satellite. The essence

of the experiment is that coherent CW signals on a number of frequencies across rather wide bands (up to 30%) would be transmitted, with carefully controlled phases.

Both amplitude and phase fluctuations would be measured in order to provide a rather complete statistical description of the signals arriving at the ground. First-order distributions of amplitude and phase would be generated; higher-order moments would also be generated. A common frequency standard on the ground and in the satellite (maintained by a two-way phase-comparison link) would supply the necessary reference.

Existing knowledge about scattering of transionospheric signals leads us to expect quite different results in at least three latitudinal regimes: equatorial, midlatitude, and auroral. Additional differences may be expected when the radio line-of-sight penetrates a region of on-going auroral disturbance. It would be desired to obtain measurements in all three latitudinal regimes.

CHANNEL-MODELING CONSIDERATIONS

As a basis for designing the experiment, the atmosphere from synchronous orbit to the ground was treated as a communication channel subject to analysis by linear filter theory. In this approach, the channel is represented totally by a time-varying impulse response $h(t, \tau)$ and its Fourier transform with respect to τ, the time-varying transfer function $H(t, f)$.

The problem is threefold: (1) to relate $h(t, \tau)$ and $H(t, f)$ and, particularly, their first- and second-order statistical measures to certain signal parameters; (2) to establish criteria for adequate sampling of the channel measures; and (3) to relate the channel measures to known atmospheric parameters.

To attack the problem, we relax the usual assumption (e.g., see *Daly* [1965]) that the channel statistics are stationary in frequency. Relaxation of the frequency-stationarity assumption is necessary at the frequencies of concern because of the dispersive nature of the ionosphere and the wide bandwidths used. We retain the assumption that the channel is wide sense stationary (WSS) in time, an assumption that is not fundamentally unsound and that can be tested for in practice. All the functions dealt with here, unless otherwise specified, are either complex envelopes, their Fourier transforms, or combinations thereof.

Signal and channel measures. The time-varying channel transfer function $H(t, f)$ is the complex envelope of the channel output when the input is a tone at $\omega + \Omega$, where $\omega = 2\pi f$ and $\Omega = 2\pi f_0$. That is,

$$\begin{aligned} y(t) &= \text{real output signal} \\ &= \text{Re}\{H(t, f) \exp [j2\pi(f + f_0)t]\} \end{aligned} \tag{1}$$

The time-varying channel impulse response $h(t, \tau)$ is a complex quantity, related to $H(t, f)$ by the following Fourier transformation:

$$\begin{aligned} h(t, \tau) &= \text{response at } t \text{ to an impulse at } (t-\tau) \\ &= \int H(t, f) \exp (j2\pi f\tau)\, df \end{aligned} \tag{2}$$

For a general input signal with complex envelope $x(t)$, the complex envelope of the output $y(t)$ is obtained through the convolution relation

$$y(t) = \int h(t, \tau)x(t - \tau)\, d\tau \tag{3}$$

Since $h(t, \tau)$ and $x(t)$ may be random variables, we are interested in various statistical measures of $y(t)$. Denoting expectation by $\langle\ \rangle$, we have

$$\langle y(t)\rangle = \int \langle h(t, \tau)\rangle\langle x(t - \tau)\rangle\, d\tau \tag{4}$$

The corresponding expressions for $Y(f)$ and $\langle Y(f)\rangle$, the Fourier transforms of $y(t)$ and $\langle y(t)\rangle$, are much more complicated; for instance,

$$\langle Y(f)\rangle = \iint \langle H(t, f')\rangle\langle x(f')\rangle \exp [j2\pi(f' - f)t]\, dt\, df' \tag{5}$$

That is, the spectral properties of the output signal involve both frequency and time properties of the channel.

Let us now turn to the second-order signal and channel measures. For a general signal $x(t)$, the time autocorrelation function is

$$R_x(\alpha, t) = \langle x^*(t - \alpha/2)x(t + \alpha/2)\rangle \tag{6}$$

The frequency autocorrelation function is defined as

$$R_X(f, \nu) \triangleq \langle X^*(f - \nu/2)\, X(f + \nu/2)\rangle \tag{7}$$

where $*$ denotes the complex conjugate. The $R_X(f, \nu)$ can be shown [*Daly*, 1965] to be the double Fourier transform of $R_X(\alpha, t)$, the time autocorrelation function. That is,

$$R_X(f, \nu) = \iint R_x(\alpha, t) \exp [-j2\pi(f\alpha + \nu t)]\, dt\, d\alpha \tag{8}$$

Two other functions (the energy density $S(f, t)$ and the ambiguity function $\psi(\alpha, \nu)$ are the two (alternate) intermediate forms in the double transform pair

$$R_X(\alpha, t) \rightleftarrows R_X(f, \nu) \tag{9}$$

The following diagram depicts the relationships between second-order signal measures:

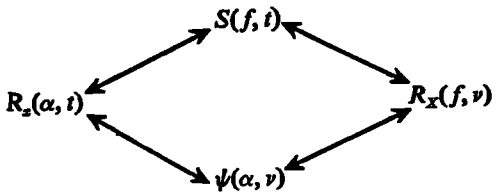

A similar set of measures exists for the (temporally WSS) channel. The channel time-and-delay autocorrelation function is

$$R_h(\alpha, \tau, \sigma) = \langle h^*(t - \alpha/2, \tau - \sigma/2)h(t + \alpha/2, \tau + \sigma/2)\rangle \tag{10}$$

The $R_h(\alpha, \tau, \sigma)$ is related to the channel time-and-frequency autocorrelation function by a double Fourier transform, as follows:

$$R_H(\alpha, \nu, f) = \iint R_h(\alpha, \tau, \sigma) \cdot \exp[-j2\pi(\nu\tau + f\sigma)]\, d\tau\, d\sigma \tag{11}$$

$$= \langle H^*(t - \alpha/2, f - \nu/2) \cdot H(t + \alpha/2, f + \nu/2)\rangle \tag{12}$$

Frequency nonstationarity requires explicit retention of the variable f in the above. If the channel were statistically stationary in frequency, $R_H(\alpha, \nu, f)$ would reduce to $R_H(\alpha, \nu)$.

By Fourier-transforming with respect to the variables in (11) and (12), six other second-order measures may be obtained. All eight measures are indicated schematically in Figure 1.

Let us turn now to the relation between input and output second-order signal measures. One of many such relations is

$$R_y(\alpha, t) = \iint R_h(\alpha, \tau, \sigma)R_x(\alpha - \sigma, t - \tau)\, d\tau\, d\sigma \tag{13}$$

When $\alpha = 0$, the above specializes to the mean-square output:

$$\langle |y(t)|^2\rangle = R_y(0, t) = \iint R_h^*(0, \tau, \sigma)R_x(\sigma, t - \tau)\, d\tau\, d\sigma \tag{14}$$

Although a great many first- and second-order channel and signal measures exist, they are intimately related through Fourier transforms and convolutions; therefore, we need only obtain one first-order and one second-order channel measure in order to characterize the atmospheric channel. The others can then be calculated, as can the measures of arbitrary signals.

For our multiple-tone experiment, the most straightforward channel measures are $\langle H(t, f)\rangle$ and $R_H(\alpha, \nu, f)$. The former (which would be obtained by averaging the complex envelope of the received tones over times where statistical stationarity holds) characterizes the channel's deterministic filter function. The latter, to be obtained from (12), characterizes the channel as a random process.

The design problem, then, reduces to ensuring adequate measurement of the channel's time-varying transfer function $H(t, f)$. 'Adequate measurement' is that which allows calculation of the channel's time and frequency autocorrelation function $R_H(\alpha, \nu, f)$ without assuming statistical stationarity in frequency.

Sampling grids and signal confinement in the ν-f plane. In a multiple-tone experiment, the time-varying transfer function $H(t, f)$ would be sampled at discrete points in the frequency domain. For obtaining $H(t, f)$ from the received signals, we would have a posteriori control of the time-sampling interval but not of the sampling interval in the frequency domain. Thus we must be reasonably certain that the sampling 'rate' in frequency is adequate and that

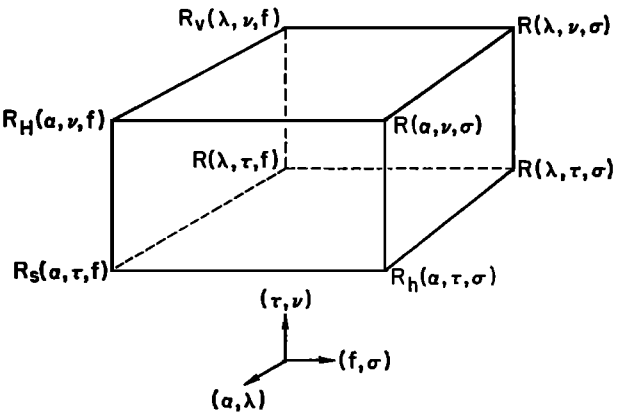

Fig. 1. Fourier transform relationships between second-order channel measures.

the sampled interval covers the bandwidths of signals of interest.

For determination of $R_H(\alpha, \nu, f)$, in the frequency-nonstationary case, both ν and f spans must be considered. Each pair of sample points in f leads to a pair of sample points in the ν direction (at $\pm\nu_0$, where ν_0 is the frequency spacing). Figure 2 shows a sampling grid in the ν–f plane for a finite space in the f direction, which results in a diamond-shaped sampling area. It can be shown [*Fremouw,* 1969] that the second-order measure $R_X(f, \nu)$ for signals that are effectively time- and/or band-limited is also confined mainly to a diamond-shaped area in the ν–f plane. Indeed, whatever the second-order measure, a similar confinement exists.

Relation of channel measures to propagation and scattering parameters. Let us suppose for the moment that the trans-atmospheric channel has simply a variable group delay $T(t)$. Then the received field due to a transmitted tone at $\omega + \Omega$ will be

$$E_0 \exp \{j[\omega + \Omega][t - T(t)]\} \tag{15}$$

so that

$$H(t, f) = E_0 \exp [-j(\omega + \Omega)T(t)] \tag{16}$$

by definition. Thus, if the E_0 factor is dropped,

$$\begin{aligned} \langle H(t, f)\rangle &= \langle \exp [-j(\omega + \Omega)T(t)]\rangle \\ &= X_T{}^*(\omega + \Omega) \end{aligned} \tag{17}$$

where X_T is the characteristic function [*Parzen,* 1960] of $T(t)$.

If $T(t)$ is a Gaussian random variable with mean T_0 and variance $\sigma_T{}^2$, then

$$\langle H(t, f)\rangle = \exp [-j(\omega + \Omega)T_0] \exp [-\tfrac{1}{2}(\omega + \Omega)^2\sigma_T{}^2] \tag{18}$$

If $\frac{1}{2}(\omega + \Omega)^2\sigma_T{}^2$ is appreciably larger than unity, the assumed channel will be a zero-mean random channel. The rms variation in ionospheric total-electron content $\sigma_{\Delta NT}$ required to make $\Omega\sigma_T$ equal to unity for three frequencies of interest is:

f, MHz	$\sigma_{\Delta NT}$, m^{-2}
400	0.48×10^{15}
1500	1.8×10^{15}
3200	3.8×10^{15}

The above values of $\sigma_{\Delta NT}$ are about 1% of typical contents; thus we expect to be on the borderline of a zero-mean random ionospheric channel.

The troposphere will also introduce a variable delay. The extra delay due to the troposphere is

$$T = \frac{10^{-6}}{c} \int_{\text{path}} n'\, ds \tag{19}$$

where n' is the refractivity, defined by

$$n = 1 + n' \times 10^{-6} \tag{20}$$

where n is the refractive index. Again, for $\Omega\sigma_T$ equal to unity, the following values of the rms variation in integrated refractivity $\int n'\, ds$ apply:

f, MHz	$\sigma_{\Delta n'T}$, n' units
400	1.2×10^5
1500	0.32×10^5
3200	0.15×10^5

A typical value of integrated refractivity for a vertical path and a (typical) surface refractivity of 400 n' units is $\int n'\, ds \approx 3 \times 10^6$. Comparing with the above values of $\sigma_{\Delta n'T}$, we see that again a 1% fluctuation puts the channel approximately on the border of being a zero-mean channel.

The time scale of the atmospheric changes is also an important parameter. In general, the larger changes may be expected to be slower. It may be, therefore, that over an observing period of interest, such as several minutes, $\langle H(t, f)\rangle$ is reasonably constant (implying temporal stationarity of the channel) and non-zero. In any case, slow variations would be 'filtered' out, if only to remove the effects of satellite motions. The frequency dependence of $\langle H(t, f)\rangle$ contains a measure of ionospheric dispersion.

The above pertains to gross (or non-scattering) effects of the atmosphere. We will now discuss scattering effects arising from spatial irregularities in atmospheric refractive index.

Consider the simple atmospheric model of a one-dimensional phase-modulating screen [*Hewish,* 1951]. Let us express the spatial distribution of a monochromatic output wave of frequency f on a

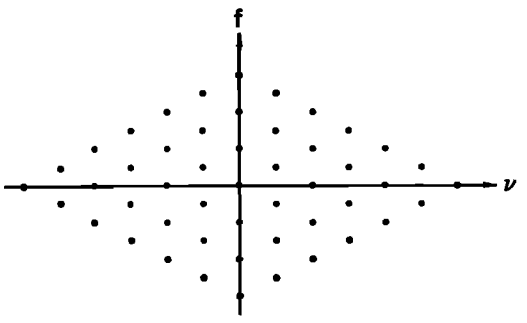

Fig. 2. Sampling matrix in the ν plane for a uniform comb of seven frequencies.

plane at time t by $e(t, f, x)$. Then each component of the spatial Fourier transform of $e(t, f, x)$ (which we shall denote by $E(t, f, S)$ can be interpreted as arising from two plane waves propagating at equal angles (given by $\theta = \sin^{-1} S$) to the normal to the plane [*Booker and Clemmow*, 1950]. The function $E(t, f, S)$ represents an angular spectrum of plane waves, and the field at any point beyond the plane can be determined from the angular spectrum [*Ratcliffe*, 1956].

If the initial plane is at the output of a distant scattering region, each pair of side waves will travel an extra distance, compared with the non-scattered wave. The corresponding extra delay at normal incidence is given by

$$\delta t = (R/c)[(1 - S^2)^{-1/2} - 1] \cong \frac{R\theta^2}{2c} \quad \text{for} \quad S^2 \ll 1 \tag{21}$$

where R is the range and c is the velocity of light.

Assuming spatial and temporal stationarity, let us suppose that the phase of $e(t, f, x)$ is normally distributed with zero mean and variance ϕ_m^2 at the initial plane and has a Gaussian autocorrelation function,

$$\rho(\xi) = \exp -(\xi/\xi_0)^2 \tag{22}$$

where ξ is the spatial shift distance and ξ_0 is the 'irregularity scale-size.' Then, with λ = the free-space wavelength, the mean of the angular spectrum for $|e| = 1$ is

$$\langle E(f, S)\rangle = \delta(S) \tag{23}$$

and the angular power spectrum [*Bramley*, 1955] is

$$\langle |E(f, S)|^2\rangle = [\exp(-\phi_m^2)] \cdot \left\{\delta(S) + \sqrt{\pi}\frac{\xi_0}{\lambda}\sum_{n=1}^{\infty}\frac{\phi_m^{2n}}{n!\,(n)^{1/2}}\exp -\left[\pi^2\frac{\xi_0^2}{\lambda^2}\frac{S^2}{n^2}\right]\right\} \tag{24}$$

The first term of (24) corresponds to the non-scattered component; therefore, the scattering reduces the power in the non-scattered component by $4.34\phi_m^2$ decibels. The angular extent of (24) is approximately

$$\theta_m = (\lambda/\xi_0)\phi_m \quad \text{for} \quad \phi_m^2 \gg 1 \quad \text{(strong scatter)}$$
$$\theta_m = (\lambda/\xi_0) \quad \text{for} \quad \phi_m^2 \ll 1 \quad \text{(weak scatter)} \tag{25}$$

In addition to the explicit frequency dependence in (24) there is a further dependence in the case of ionospheric scattering, since $\phi_m \sim 1/f$ owing to the dispersive nature of ionospheric propagation. This demonstrates the need to account for frequency nonstationarity.

Inserting (25) into (21), we find a δt corresponding to θ_m:

$$\delta t_m = (R/2c)(\lambda\phi_m/\xi_0)^2 \quad \text{(strong scatter)}$$
$$\delta t_m = (R/2c)(\lambda/\xi_0)^2 \quad \text{(weak scatter)} \tag{26}$$

which is approximately the maximum value of δt. The resulting value is also the approximate extent of $R_h(\alpha, \tau, \sigma)$ in the τ direction, which follows from consideration of the relationships between the first- and second-order means of the angular spectrum and the various channel transfer functions.

Actually, $R_h(\alpha, \tau, \sigma)$ involves the response of the channel to all frequencies, but we must restrict attention to a band around the center frequency of interest for straightforward interpretation of δt_m. This is another aspect of the difficulty in dealing analytically with nonstationarity in frequency. Since our goal is to measure the channel characteristics, however, we are primarily interested here in ensuring that we have sufficient measurement capability. Thus we shall take δt_m to be the extent of $R_h(\alpha, \tau, \sigma)$ in τ (which we shall call τ_m) for establishing the required frequency spacing of the transmitted tones. This involves simply an application of the sampling theorem.

Suppose the function $R_H(\alpha, \nu, f)$ is sampled at points on the matrix shown in Figure 3*a*. The sampled version of $R_H(\alpha, \nu, f)$ is the two-dimensional Fourier transform of the convolution of $R_h(\alpha, \tau, \sigma)$ and the 'bed-of-nails' function consisting of δ functions at the points shown in Figure 3*b*. The function $R_h(\alpha, \tau, \sigma)$ is non-zero only for $\tau \geq 0$ by the condition of causality; if we assume that its τ extent is limited to τ_m and that the extent in the σ direction is small compared with that in the τ direction, the maximum sampling interval in ν must therefore be $\nu_s = 1/\tau_m$. (This condition would be violated only for extreme nonstationarity in frequency, which is not anticipated and which can be tested for experimentally.)

Setting $\tau_m = \delta t_m$, we have

$$\nu_s = (2c/R)(\xi_0/\lambda\phi_m)^2 \quad \text{(strong scatter)}$$
$$\nu_s = (2c/R)(\xi_0/\lambda)^2 \quad \text{(weak scatter)} \tag{27}$$

Equation 27 establishes the criterion for frequency spacing in our multiple-tone experiment, in terms of

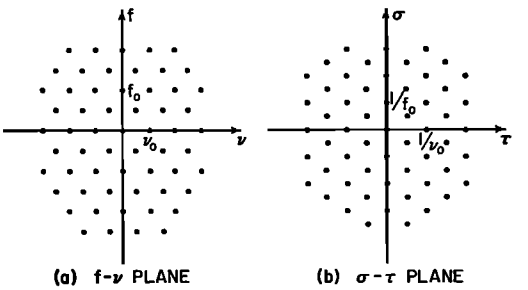

Fig. 3. Corresponding diagonal 'bed-of-nails' functions.

atmospheric-scattering parameters. We shall make quantitative use of it in the next section.

EXPERIMENT DESIGN

Because of the essentially engineering orientation of the experiment, the primary observing frequencies chosen are located at low UHF, at *L* band, and at *S* band. To relate results to known characteristics of ionospheric structure (gleaned from scintillation observations in the VHF tracking band of the National Aeronautics and Space Administration) a single VHF tone would also be transmitted. An HF tone also would be included for comparison with existing scintillation observations made at 20 and 40 MHz by various workers. It is believed that the HF and VHF tones, possibly in conjunction with those at low UHF, would provide scientifically interesting ionospheric results, in addition to engineering results.

With the primary frequency regimes set, the frequency-selection problem is reduced to a choice of the over-all bandwidth for each band and the spacings between tones within each band. The bandwidth desired is that which is likely to test the limits of usable information on the bandwidth, based on estimates of atmospheric parameters. The desired spacing would permit measurement of the channel time-varying transfer function with sufficient frequency density to calculate the time-and-frequency autocorrelation function under conditions of significant atmospheric scattering. Both deterministic and random channel parameters must be considered.

Average and slowly varying phase distortion depends almost solely on total electron content along the ray path and only negligibly on large-scale gradients. Figure 4 shows the bandwidth dependence of dispersive distortion for the three prime frequency regimes of the experiment. The abscissa $\delta\phi$ is the relative phase between the sum of a pair of equally spaced 'side bands' and their 'carrier', which is a common measure of dispersion [*Eshleman,* 1960]. The ordinate f_m is spacing between the carrier and the side band. For each of the frequency regimes (UHF (400 MHz), *L* band (1450 MHz), and *S* band (3200 MHz)) three curves of $\delta\phi$ versus f_m are shown. The curves are for 'strong' (total content of 10^{18} electrons/m^2), 'average' (10^{17}), and 'weak' (10^{16}) ionosphere conditions.

A widely used criterion for separating 'acceptable' from 'unacceptable' dispersion is the condition $\delta\phi = 1$ radian [*Eshleman,* 1960]. For the experiment under design, it is desirable to choose frequency spacings within the various bands that approximately bracket the condition $\delta\phi = 1$ under average and/or maximum ionospheric conditions. This condition is not crucial, but approximating it is desirable to ensure useful measurement of the 'usable bandwidth of the ionosphere' under varying geophysical conditions. It is of more fundamental importance to have frequencies sufficiently narrowly spaced to resolve possible ambiguities in $\delta\phi$ under maximum ionosphere conditions and to have frequencies sufficiently widely spaced to provide useful measurement accuracy of $\delta\phi$ under minimum conditions.

Initial (tentative) selection of frequencies within the three primary bands was made to provide triplets (a 'carrier' plus two 'side bands') that would meet the conditions described above for measurement of $\delta\phi$. The selected frequencies were then ad-

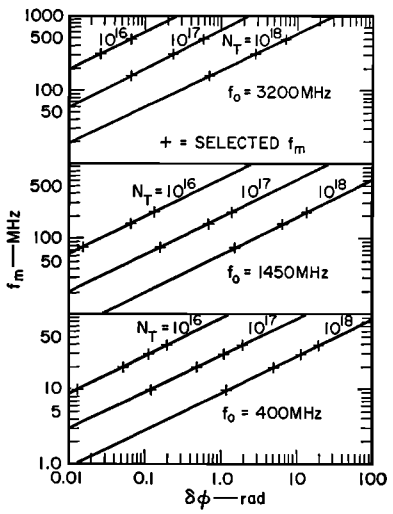

Fig. 4. Side band-pair-to-carrier frequency spacing f_m for various frequency regimes and ionospheric columnar electron contents.

justed to provide the sampling combs needed for determination of the channel time-and-frequency autocorrelation function under conditions of random scatter. The transmission spectrum selected is shown in Figure 5. The corresponding values of f_m are represented in Figure 4 by crosses on the curves.

The required frequency spacing ν_s is related to ionospheric scattering parameters through (27). Figure 6 shows plots of irregularity scale size ξ_0 versus rms phase deviation ϕ_m imposed by ionospheric scattering as calculated from (27) for the three frequency spacings employed in the spectrum shown in Figure 5. A range R of 1000 km from scattering layer to receiver was assumed. (Ionospheric irregularities typically lie at heights of a few hundred kilometers.) The curves show the boundary, for the three bands, between combinations of irregularity scale ξ_0 and the square root of the ionospheric optical depth for scattering [*Fremouw,* 1966], ϕ_m, whose effects can be accurately sampled, and those for which only an upper limit on coherence bandwidth can be ascertained. The boundary is only approximate, since it is based on a simplified but tractable model. The region above and to the left of the curves in Figure 6 is the region of accurate sampling.

Commonly occurring ionospheric irregularities have values for ξ_0 of the order of 1000 meters and produce values for ϕ_m considerably smaller than unity in all three bands. Note that such values lie well above and to the left of the curves. Under conditions of line-of-sight aurora, values of ξ_0 of the order of 100 meters may be expected [*Fremouw,* 1966], and ϕ_m may occasionally exceed unity in the low UHF band. Under such extreme conditions, only an upper limit on coherence bandwidth will be measured at UHF. For observations under such

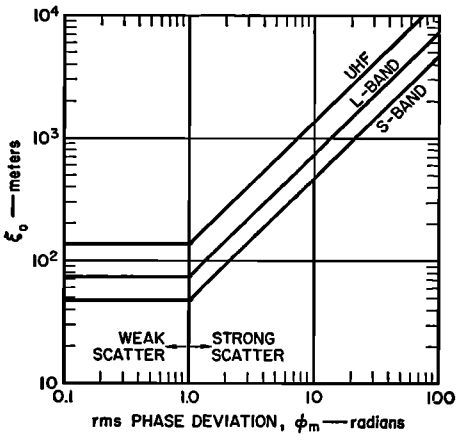

Fig. 6. Boundaries between fully assessable (upward and left) combinations of irregularity scale, ξ_0 and ionospheric optical depth for scattering, ϕ_m^2 and combinations whose effects can be measured only as limiting values (downward and right).

conditions, which are of considerable operational as well as scientific interest, ten tones are planned for the UHF comb rather than just the seven planned for L and S bands.

It is not anticipated that ϕ_m will reach unity at L and S bands even under extreme auroral conditions. It is under such conditions that measurable ionospheric scattering effects are most likely to be observed at the higher frequencies, and the resulting data will be available for further refined estimates of the coherence bandwidth at UHF. It is therefore not considered desirable to design the experiment for the expected worst auroral (and probably equatorial) case at UHF at the expense of reduced information under more commonly occurring conditions or of considerably greater experimental complexity and added power.

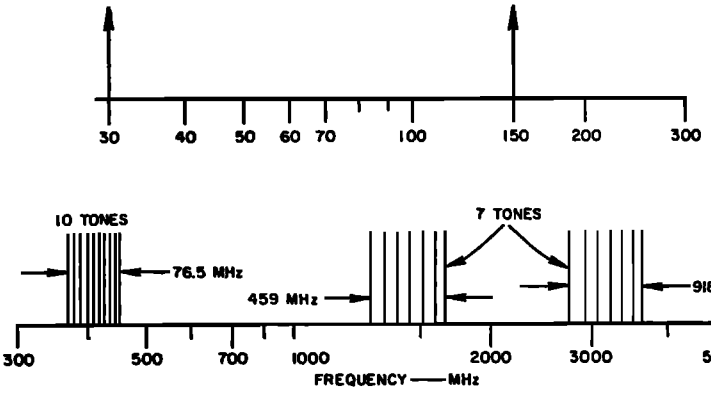

Fig. 5. Desired satellite transmission spectrum.

Aside from frequency selection, the prime design parameters are the phase stability and the system signal-to-noise ratio. Existing scintillation measurements at individual frequencies were used to establish stability needs, transmitter power requirements, necessary antenna gains, etc. The interested reader is referred to *Fremouw* [1969] for instrumental details.

CONCLUSION

The experiment described in this paper is in the design stage. It has been found necessary to resort to rather advanced techniques for the satellite transmitter. In general, the experiment has been found to be ambitious but not infeasible. It is currently hoped that the transmitter will be launched into geostationary orbit in 1972. However, no firm commitment for a launch has been made as of this writing, and so the plans described above should be considered tentative. It is possible that actual implementation could be more modest than the described plan.

The wide-band nature of the experiment has been stressed here. We also hope to make spaced receiver measurements at several frequencies for determining signal spatial autocorrelation functions. It is hoped that both spatial and time-frequency measurements will be useful to system designers. In addition, interpretation of measurement results should provide insights into atmospheric processes that are of geophysical interest. The purpose of describing the proposed experiment at this time is to call the attention of both the communications and aeronomy communities to the hoped-for results. In particular, it is intended to describe it so that plans may be made in time for useful coordinated observations between various interested groups.

Acknowledgment. This work was supported by the Defense Atomic Support Agency, under contract DASA01-68-C-0104.

REFERENCES

Booker, H. G., and P. C. Clemmow (1950), The concept of an angular spectrum of plane waves and its relation to that of a polar diagram and an aperture distribution, *Proc. IEE, London, 97, Pt. 3,* 11–17.

Bramley, E. N. (1955), Some aspects of the rapid directional fluctuations of short radio waves reflected at the ionosphere, *Proc. IEE, London, 102, Pt. B,* 533–540.

Coates, R. J., and T. S. Golden (1968), Ionospheric effects on telemetry and tracking signals from orbiting spacecraft, *Rep. X-520-68-76,* Goddard Space Flight Center, Greenbelt, Maryland.

Daly, R. F. (1965), Signal design for efficient detection in randomly dispersive media, *Rep. SRI Sponsored Res., Project 186531-144,* Stanford Research Institute, Menlo Park, California.

Eshleman, V. R. (1960), On the band width of the ionosphere, in *Effects of the Atmosphere on Radar Resolution and Accuracy, Part XIII of Final Report,* edited by A. M. Peterson, SRI Project 2225, Stanford Research Institute, Menlo Park, California.

Flood, W. A. (1963), A study of radio-star fadeouts and their application to radar resolution, *J. Geophys. Res., 68,* 4129–4140.

Fremouw, E. J. (1966), Radio wave scattering structure in the disturbed auroral ionosphere: Some measured properties, *Rep. UAG R-180,* Geophysical Institute of the University of Alaska, College, Alaska.

Fremouw, E. J., editor (1969), An experiment to measure trans-atmospheric wide-band radio propagation parameters, *Final Rep., Phase 1, SRI Proj. 7161,* Stanford Research Institute, Menlo Park, California.

Fremouw, E. J., and J. M. Lansinger (1968), Radio-star visibility fades in Alaska near solar minimum, *J. Geophys. Res., 73,* 3565–3572.

Hewish, A. (1951), The diffraction of radio waves in passing through a phase-changing ionosphere, *Proc. Roy. Soc. London, A, 209,* 81–96.

Koster, J. R. (1958), Radio-star scintillations at an equatorial station, *J. Atmos. Terr. Phys., 12,* 100–109.

Little, C. G., G. C. Reid, E. Stiltner, and R. P. Merritt (1962), An experimental investigation of the scintillation of radio stars observed at frequencies of 223 and 456 megacycles per second from a location close to the auroral zone, *J. Geophys. Res., 67,* 1763–1784.

Parzen, E. (1960), *Modern Probability Theory and Its Applications,* John Wiley, New York.

Ratcliffe, J. A. (1956), Some aspects of diffraction theory and their application to the ionosphere, *Rep. Progr. Phys., 19,* 188–266.